Evaluation of Hydrodynamic Performance of Quarter Circular Breakwater Using Soft Computing Techniques

N. Ramesh, A. V. Hegde and Subba Rao

Abstract Breakwaters are massive structures constructed to provide the required tranquility within the ports. They are also used for safeguarding the beaches from eroding due to the severe action of waves, especially during inclement weather. In recent years, innovative structures such as Semi-circular and Quarter-circular Breakwaters (QBW) are being evolved to fulfill the ever-increasing demand from the coastal sector. QBW is a caisson with quarter circular surface towards incident waves, with horizontal bottom and a vertical wall on its rear side placed on a rubble mound foundation. In this paper, the experimental data collected at National Institute of Technology, Surathkal is used. The data collected is analysed by plotting the non-dimensional graphs of reflection coefficient, reflected wave height and incident wave height for various values of wave steepness. The values are used for prediction of QBW adopting Multi-Layer Perceptron (MLP) and Radial Basis Function (RBF) networks. Goodness-of-Fit (GoF) test using Kolmogorov–Smirnov (KS) test statistic is applied for checking the adequacy of MLP and RBF networks to the experimental data. The performance of these networks is evaluated by using Model Performance Indicators (MPIs), viz. correlation coefficient, mean absolute error and model efficiency. The GoF test results and values of MPIs indicated the MLP is better suited amongst two networks adopted for evaluation of hydrodynamic performance of QBW.

Keywords Correlation coefficient · Kolmogorov–Smirnov test
Mean absolute error · Model efficiency · Multi-layer perceptron
Quarter-circular breakwater · Radial basis function

N. Ramesh (✉) · A. V. Hegde · S. Rao
National Institute of Technology Karnataka, Surathkal, Mangalore 575025, Karnataka, India
e-mail: rameshen@yahoo.com; 10ramesh64@gmail.com

S. Rao
e-mail: surakrec@gmail.com

K. Murali et al. (eds.), *Proceedings of the Fourth International Conference in Ocean Engineering (ICOE2018)*, Lecture Notes in Civil Engineering 23,
https://doi.org/10.1007/978-981-13-3134-3_7

1 Introduction

Breakwater is a structure generally, used in coastal protection works and also for creating tranquility in basin in harbors. Over the years, breakwater was of rubble mound weighing in tons. In the latter part of nineteenth-century innovative structures like tetrapods, tripods and other interlocking blocks are also evolved. Considering the huge quantity of rock material required, at the beginning of twenty-first century caisson type of breakwater were thought off. One such breakwater is Quarter-circular Break Water (QBW), a new-type breakwater first proposed by Xie et al. [15] on the basis of Semi-circular Break Water (SBW). The QBW is usually placed on rubble mound foundation and its superstructure consists of a quarter circular surface facing sea sides, a horizontal bottom and a rear vertical wall. The QBW structure is hollow, hence, the weight and materials required are less and it is more suitable where the foundation is relatively weak. The QBW is a prefabricated caisson, which can be properly designed for handling stresses and can be transported and placed with more precision at the desired location. Depending upon the purpose the Quarter-circle breakwater may be fabricated as emerged or submerged type structure, with and without perforation to dissipate the incident wave energy.

2 Literature Review

Jiang et al. [9] studied the performance of QBW by comparing the hydraulic performances of SBW and QBW under similar hydraulic conditions. They conducted 2-Dimensional (2D) vertical wave numerical model and physical model studies, and found that wave reflection of both QBW and SBW are closer to each other. They stated that the wave reflection coefficient (K_r) remains almost same with values less than 1.0 even when freeboard (h_c) value becomes 2–3 times incident wave height (H_i) for both types of breakwaters. During wave overtopping in submerged condition, they found high flow velocity and vortexes near the rear walls of QBW, which may be due to the top sharp corner and sudden expansion of flow around QBW. They described that the flow fields in front of both QBW and SBW are similar in both in submerged as well as emerged conditions and this explains the closeness of reflection coefficient values for both breakwaters.

Shi et al. [13] studied the hydrodynamic performance of QBW under both regular and irregular wave conditions. Regular waves were generated by reciprocating wave paddle at a constant speed, whereas irregular waves were generated by frequency spectrum simulation with target spectrum of JONSWAP type. For analyzing the wave reflection, two types of wave reflection coefficients were described by Shao [12], viz. (i) K_r that describes the whole effect of wave reflection by breakwater and (ii) Circular-surface reflection coefficient (K_{rc}) that describes the reflective effect by circular surface on the adjacent flow field in front of the breakwater. The study revealed that at the same relative freeboard height (h_c/H_i), the value of K_r was higher

than K_{rc} that indicates the entire reflective effect of QBW is stronger than that by the circular surface on the adjacent flow field. To estimate the energy dissipation as the wave passes over the breakwater wave energy loss parameter (K_{Eloss}) was described. K_{Eloss} is the ratio of dissipated wave energy to the original gross wave energy within the process of wave structure interaction. Based on the results obtained from the study, it was found that the loss of wave energy for emerged breakwater is larger than that for submerged breakwater.

Hegde and Ravikiran [8] conducted experiments on the physical model of QBW in 2D wave flumes to evaluate the reflection characteristics of QBW of different radii in different submergence conditions. The models were made of galvanized iron sheets and coated with a cement slurry to simulate concrete surface. For finding the variation of K_r different graphs were plotted with the incident wave steepness (H_i/gT^2) (where, g is the gravitation and T is the wave period) for various submergence ratios (d/h_c) and different ranges of (R/H_i) (where, d is the depth of water and R is the breakwater radius). For all values of d/h_c and R/H_i, they found that K_r increases logarithmically (best-fit) as incident wave steepness increases. The study revealed that whatever may be the depth, caisson radius, height of structure crest (from seabed) steeper the waves the more will be the reflection from breakwater. Hafeeda et al. [7] conducted experiments in a 2D monochromatic wave flume on a seaside perforated QBW model. They analyzed the experimental data by plotting the non-dimensional graphs of K_r (i.e., H_r/H_i) (where H_r is the reflected wave height) for various values of R/H_i. They observed that the value of K_r increased with increase in wave steepness and when the freeboard (h_c) increased then the value of K_r also increased. They found that when the height of the structure (h_s) increases, a smaller height of the QBW portion of the caisson is exposed to waves, which is the effect of the curvature is less pronounced that tend to lesser dissipation and more reflection.

Binumol et al. [3] conducted physical model studies of QBW with three different radii and S/D (spacing to the diameter of perforations) ratio. Dimensional analysis was carried out to find the non-dimensional parameters such as incident wave steepness, depth parameter (d/gT^2), height of structure, depth of water, wave run up (R_u/H_i), wave rundown (R_d/H_i), etc., using Buckingham's π-theorem. The experimental data collected was analyzed by plotting the graph of dimensionless wave run up and dimensionless wave rundown for various values of wave steepness and different heights of structure to the depth of water. They observed that the value of R_u/H_i increases with an increase in wave steepness for all values of h_s/d and d/gT^2. This was because as wave height increases there is an increase in wave energy and hence run up increases with an increase in wave steepness. For all values of h_s/d and d/gT^2, the dimensionless wave rundown was found to decrease with increase in wave steepness for all values of h_s/d and d/gT^2 because as wave height increases there is an increase in wave energy resulting in more run up and hence less rundown. R_d/H_i was also found to increase with the increase in the depth parameter (d/gT^2), because at higher water depths the effect of curvature is more pronounced resulting in lower run up and hence more wave rundown. Balakrishna and Hegde [2] investigated reflection coefficient (K_r) and dissipation (or loss) coefficient (K_L) for physical models of quarter circle caisson breakwater for different radii with constant S/D ratio. They

observed that reflection coefficient was found to increase with wave steepness, which was similar to all earlier studies. Dissipation coefficient decreased with the increase in wave steepness. The study revealed that as wave period decreases the value of loss coefficient decreases. The study also revealed that as h_s/d increases, dissipation increases which is a reverse trend in the case of reflection, this trend is found to be true for all values of d/gT^2 values.

Generally, computational intelligence techniques, viz., Artificial Neural Network (ANN), Adaptive Neuro-Fuzzy Interface System (ANFIS), Support Vector Machine (SVM) regression, genetic algorithm, etc., have been efficaciously proposed as an efficient tool for modelling and predictions in coastal engineering problems [1]. Karthik and Rao [11] reviewed the study on the application of soft computing techniques include ANN-based Multi-Layer Perceptron (MLP) and Radial Basis Function (RBF) networks, ANFIS, SVM and Fuzzy Logic in breakwater studies. In the present study, MLP and RBF networks are used for prediction of the variables considered for evaluation of the hydrodynamic performance of QBW. Goodness-of-Fit (GoF) test using Kolmogorov–Smirnov (KS) test statistic is applied for checking the adequacy of MLP and RBF networks to the experimental (or observed) data. The performance of these networks is evaluated by using Model Performance Indicators (MPIs), viz., Correlation Coefficient (CC), Mean Absolute Error (MAE), and Model Efficiency (MEF). This paper presents the procedures adopted in evaluating the hydrodynamic performance of QBW using MLP and RBF networks with an illustrative example.

3 Methodology

Artificial Neural Network (ANN) modeling procedures adapt to the complexity of input–output patterns and accuracy goes on increasing as more and more data become available. Figure 1 shows the architecture of ANN that consists of an input layer, hidden layer, and output layer [14]. From ANN structure, it can be easily understood that input units receive data from external sources to the network and send them to the hidden units, in turn, the hidden units send and receive data only from other units in the network, and output units receive and produce data generated by the network, which goes out of the system. In this process, a typical problem is to estimate the output as a function of the input. This unknown function may be approximated by a superposition of certain activation functions such as tangent, sigmoid, polynomial, and sinusoid in ANN. A common threshold function used in ANN is the sigmoid function (f(S)) expressed by Eq. (1), which provides an output in the range of $0 \leq f(S) \leq 1$.

$$f(S) = \left[1 + \exp(-S_i)\right]^{-1} \text{ and } S_i = \sum_{i=1}^{N} I_i W_{ij} + O_i, \quad j = 1, 2, 3, \ldots, M \qquad (1)$$

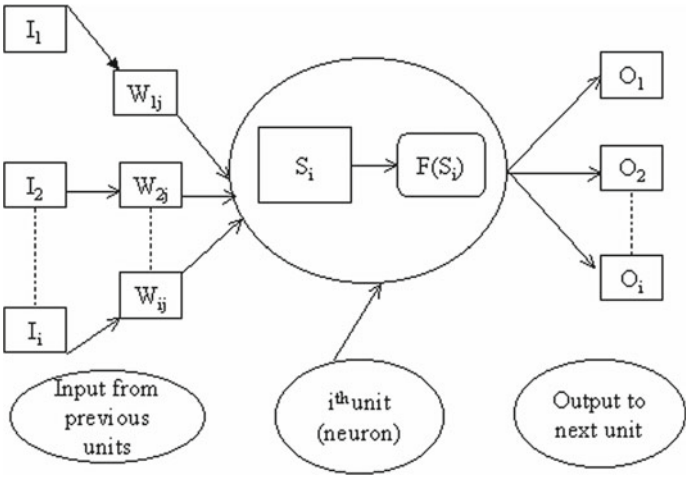

Fig. 1 Architecture of ANN

where S_i is the characteristic function of *i*th layer, I_i is the input (I) unit of *i*th layer, O_i is the output (O) unit of *i*th layer, W_{ij} is the synaptic weights between input (i) and hidden (j) layers, N is the number of observations and M is the number of neurons (or units) of hidden layer [10].

3.1 Theoretical Description of MLP Network

MLP network [6] is based on an architecture with a single hidden layer as shown in Fig. 2. Gradient descent is the most commonly used training algorithm in MLP in which each input unit of the training dataset is passed through the network from the input layer to the output layer. The network output is compared with the target output and output error (E) is computed using Eq. (2).

$$E = \frac{1}{2}\sum_{i=1}^{N}\left(X_i - X_i^*\right)^2 \tag{2}$$

where X_i is the observed value of *i*th sample and X_i^* is the predicted value for *i*th sample.

$$\Delta W_{ij}(M) = -\varepsilon\frac{\partial E}{\partial W_{ij}} + \alpha\,\Delta W_{ij}(M-1) \tag{3}$$

where $\Delta W_{ij}(M)$ is the weight increments between *i*th and *j*th layers during M neurons (units) and $\Delta W_{ij}(M-1)$ is the weight increments between *i*th and *j*th layers during

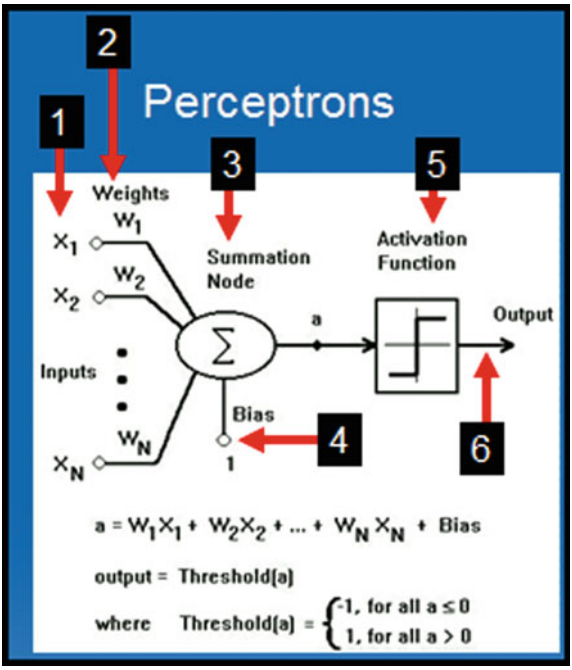

Fig. 2 Structure of MLP network

M − 1 neurons. In MLP, momentum factor (α) is used to speed up training in the very flat region of the error surface to prevent oscillation in the weight and learning rate (ε) is used to increase the chance of avoiding the training process being trapped in local minima instead of global minima.

3.2 Theoretical Description of RBF Network

RBF network is supervised and three-layered feedforward neural network and presented in Fig. 3. The hidden layer of RBF network consists of a number of nodes and a parameter vector called a "centre", which can be considered the weight vector. In RBF, the standard Euclidean distance is used to measure the distance of an input vector from the center. The design of neural networks is a curve-fitting problem in a high dimensional space in RBF [10].

Training the RBF network implies finding the set of basis nodes and weights. Therefore, the learning process is to find the best fit to the training data. The transfer function of the nodes is governed by nonlinear functions that are assumed to be an approximation of the influence that data points have at the center. The transfer function of an RBF is mostly built up of Gaussian rather than sigmoid. The Gaussian function decrease with distance from the center. The transfer function of the nodes is governed by nonlinear functions that is assumed to be an approximation of the

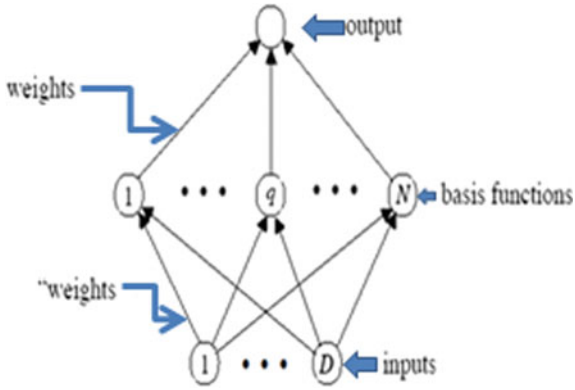

Fig. 3 Structure of RBF network

influence that data points have at the center. The Euclidean length is represented by r_j that measures the radial distance between the datum vector $\underline{X}(X_1, X_2, \ldots, X_M)$ and the radial center $\underline{X}^{(j)} = (W_{1j}, W_{2j}, \ldots, W_{Mj})$ can be written as:

$$r_j = \left\|\underline{X} - \underline{X^{(j)}}\right\| = \left[\sum_{i=1}^{M} \left(X_i - W_{ij}\right)^2\right]^{1/2} \tag{4}$$

where $r_j = \|\|$ is the Euclidean norm and $\Phi(\,)$ is the activation function. A suitable transfer function is then applied to r_j to give $\Phi(r_j) = \Phi\left\|\underline{X} - \underline{X^{(k)}}\right\|$. Finally, the output layer $(k-1)$ receives a weighted linear combination of $\Phi(r_j)$.

$$X^{(k)} = W_0 + \sum_{j=1}^{N} c_j^{(k)} \Phi(r_j) = W_0 + \sum_{j=1}^{N} c_j^{(k)} \Phi\left(\left\|\underline{X} - \underline{X^{(j)}}\right\|\right) \tag{5}$$

where, c_j is the center of the neuron in the hidden layer and $\Phi(r_j)$ is the response of the *j*th hidden unit and W_0 is the bias term [11].

3.3 Goodness-of-Fit Test

GoF test [5] involving, viz., Kolmogorov–Smirnov (KS) test statistic is applied for checking the adequacy of applying MLP and RBF networks to the series of experimental data. Theoretical description of the KS test statistic is as follows:

$$KS_C = \underset{i=1}{\overset{N}{Max}}(F_e(X_i) - F_D(X_i)) \tag{6}$$

where $F_e(X_i) = (i - 0.35)/N$ is the Empirical Cumulative Distribution Function (CDF) of X_i and $F_D(X_i)$ is the computed CDF of X_i by MLP and RBF.

3.4 Model Performance Analysis

The performance of MLP and RBF networks used in prediction of the variables (K_L, K_r, and K_t) is evaluated by Model Performance Indicators (MPIs), viz., Correlation Coefficient (CC), Mean Absolute Error (MAE) and Model Efficiency (MEF), and is given as follows:

$$\begin{aligned} \mathrm{CC} &= \frac{\sum_{i=1}^{N}\left(X_i-\overline{X}\right)\left(X_i^*-\overline{X^*}\right)}{\sqrt{\left(\sum_{i=1}^{N}\left(X_i-\overline{X}\right)^2\right)\left(\sum_{i=1}^{N}\left(X_i^*-\overline{X^*}\right)^2\right)}} \\ \mathrm{MAE}(\%) &= \left(\frac{1}{N}\sum_{i=1}^{N}\left|X_i-X_i^*\right|\right)*100 \\ \mathrm{MEF}(\%) &= \left(1-\frac{\sum_{i=1}^{N}\left(X_i-X_i^*\right)^2}{\sum_{i=1}^{N}\left(X_i-\overline{X}\right)^2}\right)*100 \end{aligned} \tag{7}$$

where $\overline{X}$ is the average value of observed data and $\overline{X^*}$ is the average value of predicted data [4]. The network with high CC, less MAE, and better MEF is considered as best suited amongst MLP and RBF networks adopted in the prediction of the variables used for evaluation of the hydrodynamic performance of QBW.

4 Application

In this paper, a study on the comparison of the hydrodynamic performance of QBW was carried out. The experimental data, viz., depth of water (d), wave period (T), incident wave height (H_i), transmitted wave height (H_t), reflected wave height (H_r), transmission coefficient (K_t), loss coefficient (K_L), wavelength (L), reflection coefficient (K_r), incident wave steepness (H_i/gT^2), relative freeboard (h_c/H_i) and relative wave height (H_i/d) collected at National Institute of Technology, Surathkal, is analysed by plotting the non-dimensional graphs of reflection coefficient, reflected wave height and incident wave height for various values of wave steepness. The values were used for prediction of QBW adopting ANN-based MLP and RBF networks.

4.1 Description of Experimental Setup

The study was conducted in the regular wave flume available in the marine structures laboratory of the Department of Applied Mechanics and Hydraulics, National Institute of Technology Karnataka, Surathkal. The experiments were performed in

a wave flume with dimensions of 50 m long, 0.74 m wide and 1.1 m deep. Out of 50.0 m, 42 m length has a smooth concrete bed. It has a 6.3 m long, 1.5 m wide and 1.4 m deep chamber at one end, where wave flap is hinged at the bottom generates waves. The flap is controlled by an induction motor of 11 kw, 1450 rpm and is regulated by an inverter drive, 0–50 Hz rotating with a speed range of 0–1550 rpm. This facility is able to generate regular waves of 0.08–0.24 m of periods 0.8–4 s. A series of vertical asbestos sheets are spaced at about 10 cm distance from each other and kept parallel to the length of the flume to dissipate the generated waves by damping the disturbance caused by successive reflection and to smoothen them. The QBW model is placed in the flume 28 m away from the wave flap, above the rubble mound foundation (Fig. 4). The slope used for the rubble foundation is 1:2. Three capacitance-type wave probes were used for measuring the incident and reflected wave heights. The wave probes were placed at a distance of 4 m from the center of the model.

In the present study, 75% of data was used for training (TRG) and 25% of data for testing (TES). Table 1 presents the descriptive statistics (i.e., Average, Standard Deviation (SD), Coefficient of Variation (CV), Coefficient of Skewness (C_S), and Coefficient of Kurtosis (C_K)) of the observed data of the variables that are considered for prediction for evaluation of the hydrodynamic performance of QBW.

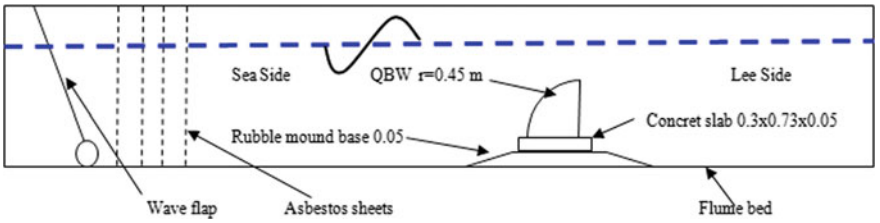

Fig. 4 A schematic diagram of experimental setup

Table 1 Descriptive statistics of the observed data

Descriptive statistics	K_L		K_r		K_t	
	Data points (1–27)	Data points (28–36)	Data points (1–27)	Data points (28–36)	Data points (1–27)	Data points (28–36)
Average	0.519	0.609	0.154	0.079	0.823	0.772
SD	0.134	0.128	0.070	0.046	0.076	0.089
CV (%)	25.8	21.0	45.3	57.9	9.3	11.5
C_S	−0.205	−0.789	−0.110	0.537	−0.329	0.602
C_K	−1.139	−1.112	0.049	−0.430	−1.249	−1.238

5 Results and Discussions

Statistical software, namely, SPSS (Statistical Package for the Social Sciences) is used to predict the hydrodynamic characteristics of QBW such as refraction coefficient, reflection coefficient, and loss coefficient using MLP and RBF. The experimental data was trained with MLP and RBF networks, which are used to determine the optimum network architecture for the variables, viz., K_L, K_r, and K_t. The determined Optimum Network Architecture (ONA) with model parameters obtained from MLP and RBF developed through REG was used for prediction of QBW.

5.1 Prediction of K_L, K_r, and K_t Using MLP

The momentum factor (α) and learning rate (ε) were fixed as 0.65 and 0.08, while optimizing the network architecture of MLP for K_L, K_r, and K_t. The network data was trained with ONA (i.e., 12-15-1) with one input layer with 12 units, one hidden layer with 15 hidden units and one output layer with 1 unit. The network was tested with model parameters for the prediction of the variables (K_L, K_r, and K_t) to evaluate the hydrodynamic performance of QBW.

5.2 Prediction of K_L, K_r, and K_t Using RBF

By using the procedures of RBF, as described in Sect. 3.2, the experimental data was trained with model parameters to determine the ONAs of K_L, K_r, and K_t. The ONAs were determined as 12-7-1 for K_L whereas 12-10-1 for K_r and 12-4-1 for K_t. The ONAs were used to test the network data of the variables considered in the study. The time series plots of predicted values of the variables (K_L, K_r and K_t) using MLP and RBF networks together with observed data are presented in Figs. 5, 6 and 7. The scatter plots of observed and predicted variables with the model fit and R^2 (Coefficient of determination) values are presented in Figs. 8, 9 and 10.

From Figs. 5, 6 and 7, it can be seen that the predicted values of the variables (K_L, K_r and K_t) using MLP network gives better performance than RBF during the testing period. From Figs. 8, 9 and 10, it can be seen that the R^2 values obtained from fitted model using MLP for K_L, K_r and K_t variables are 0.970, 0.926 and 0.980, which indicates that there is a perfect fit between the observed and predicted variables.

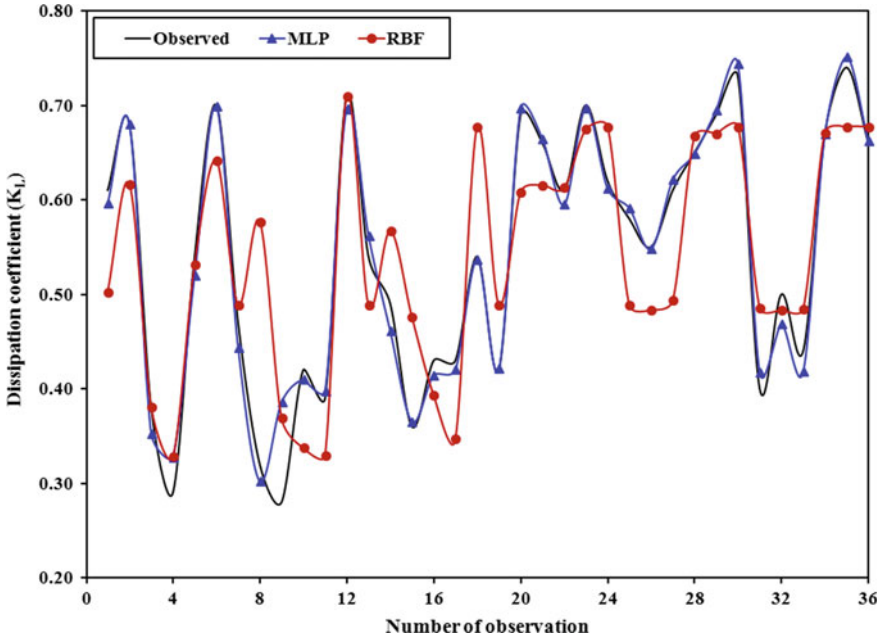

Fig. 5 Time series plots of observed and predicted values of K_L (using MLP and RBF)

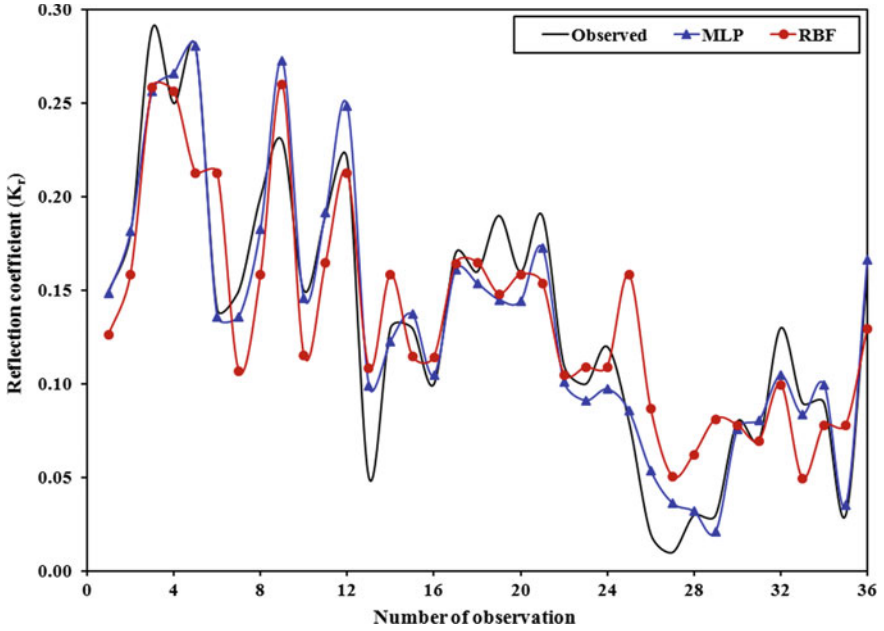

Fig. 6 Time series plots of observed and predicted values of K_r (using MLP and RBF)

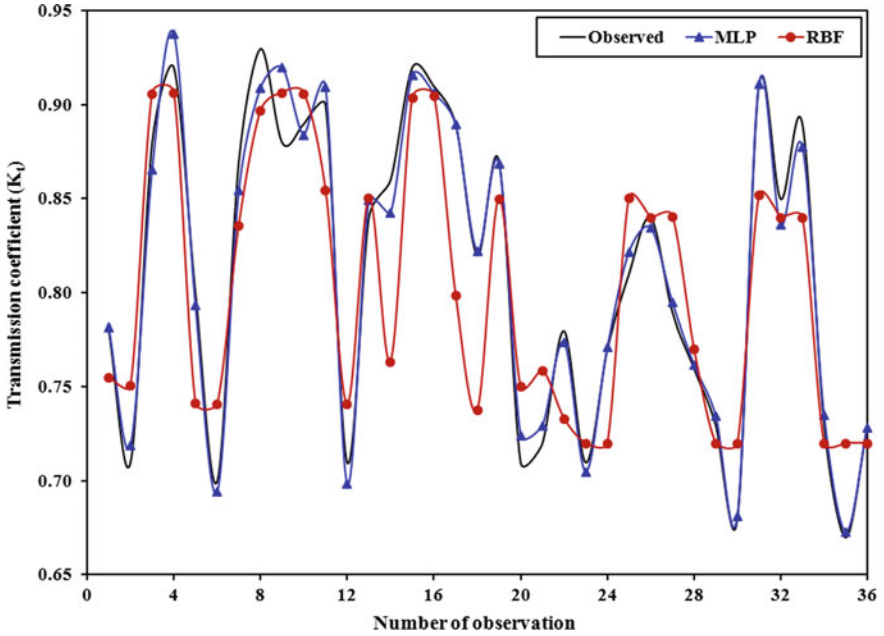

Fig. 7 Time series plots of observed and predicted values of K_t (using MLP and RBF)

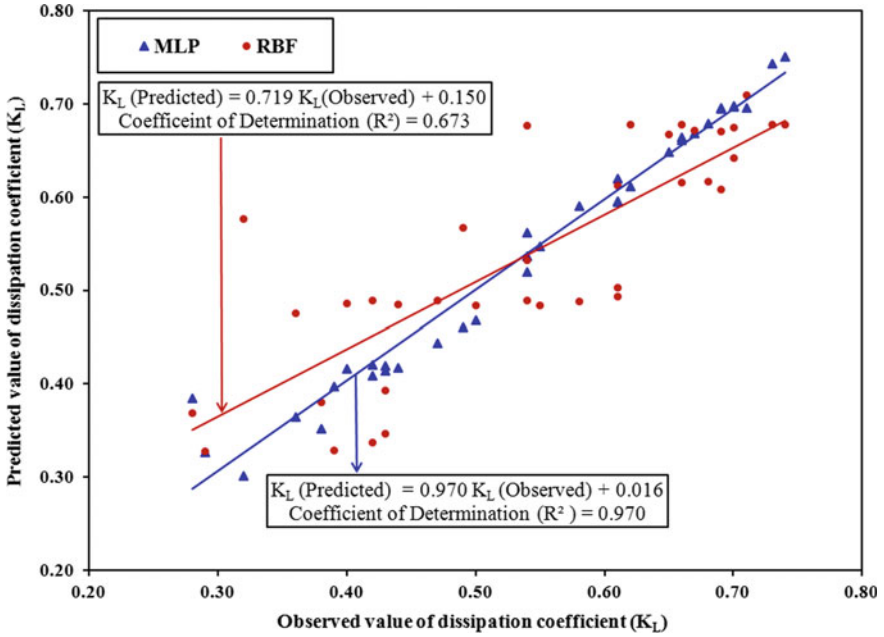

Fig. 8 Scatter plots of observed and predicted values of K_L (using MLP and RBF)

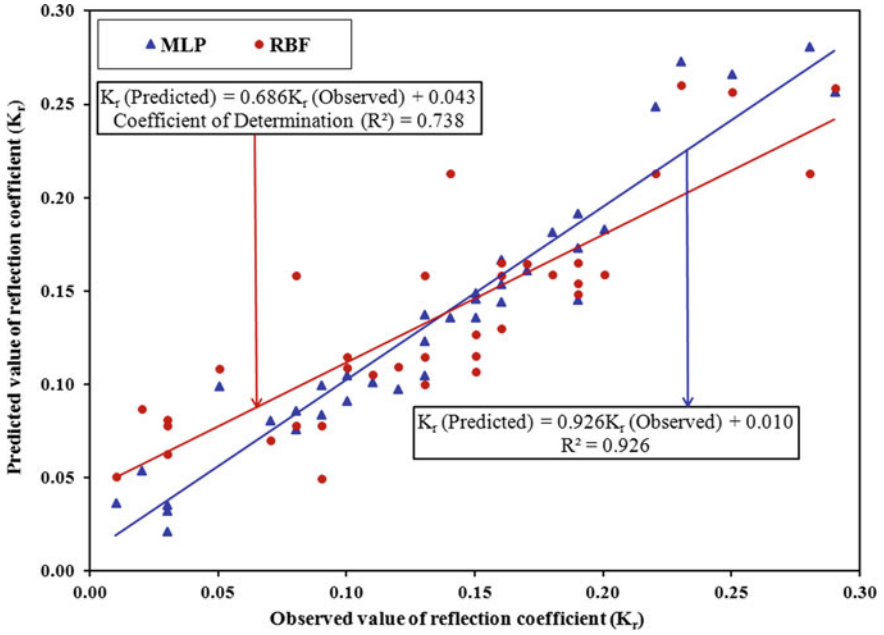

Fig. 9 Scatter plots of observed and predicted values of K_r (using MLP and RBF)

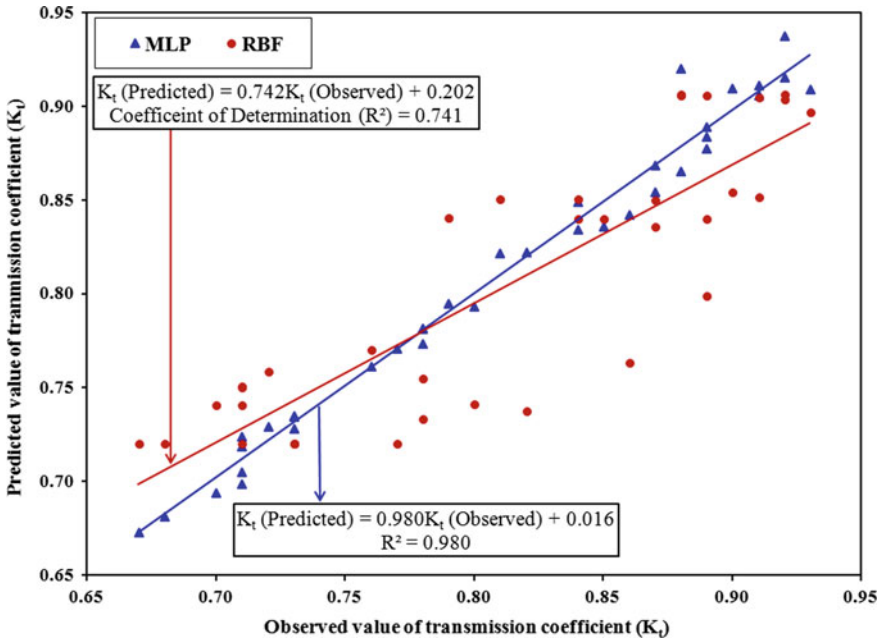

Fig. 10 Scatter plots of observed and predicted values of K_t (using MLP and RBF)

5.3 Analysis Based on GoF Test

The KS test statistic values of MLP and RBF networks for the variables K_L, K_r and K_t were computed and found to be varied between 0.125 and 0.210. These values were noted to be less than of its theoretical value of 0.221 at 5% level, and at this level, both MLP and RBF are found to be acceptable for prediction of the variables (K_L, K_r and K_t). The predicted variables were used for evaluation of the hydrodynamic performance of QBW.

5.4 Performance Analysis Based on MPIs

The model performance of MLP and RBF networks used in predication of the variables was evaluated by MPIs and the results are presented in Table 2.

From Table 2, it may be noted that the MEF obtained from MLP network is higher than the corresponding values of RBF. The CC values obtained from MLP for the predicted variables vary from 0.950 to 0.998. Also, from Table 2, it may be noted that the percentages of MAE obtained from MLP for the predicted variables (K_L, K_r and K_t) during TRG and TET periods are less than the corresponding values of RBF. From GoF test results using KS test statistic and model performance analysis using MPIs values, it was found that the MLP network is better suited amongst two networks adopted for prediction of the variables for evaluation of hydrodynamic performance of QBW.

5.5 Analysis Based on Descriptive Statistics

In addition to MPIs, the overall performance of MLP and RBF networks used in prediction of the variables (K_L, K_r, and K_t) was analyzed through the descriptive statistics (i.e., Average, Standard Deviation (SD), Coefficient of Variation (CV), Coefficient of Skewness (C_S) and Coefficient of Kurtosis (C_K)), and the results are presented in Table 3.

From the values of descriptive statistics of the variables, as given in Tables 1 and 3, the percentage of deviation on the average predicted value of K_L using MLP network with reference to the average observed value was computed as 0.6% and 0.2% for training and testing periods. Similarly, for K_r, the values were computed as 1.9% (for training) and 1.3% (for testing). For K_t, the values were computed as 0.2% (for training) and 0.1% (for testing).

Table 2 Values of MPIs for K_L, K_r, and K_t given by MLP and RBF networks

MPIs	K_L				K_r				K_t			
	MLP		RBF		MLP		RBF		MLP		RBF	
	TRG	TES	TRG	TES	TRG	TES	TRG	TES	TRG	TES	TRG	TES
CC	0.981	0.994	0.769	0.956	0.950	0.968	0.836	0.677	0.986	0.998	0.825	0.959
MAE (%)	1.6	1.2	6.8	3.5	1.6	0.9	3.0	2.7	0.9	0.5	3.7	2.7
MEF (%)	96.3	98.8	58.8	89.9	90.9	97.7	71.7	78.7	97.3	99.5	66.7	86.2

Table 3 Descriptive statistics of the predicated variables (K_L, K_r and K_t) using MLP and RBF

Descriptive statistics	K_L				K_r				K_t			
	MLP		RBF		MLP		RBF		MLP		RBF	
	TRG	TES	TRG	TES	TRG	TES	TRG	TES	TRG	TES	TRG	TES
Average	0.516	0.608	0.515	0.611	0.151	0.078	0.154	0.081	0.821	0.770	0.814	0.767
SD	0.129	0.135	0.119	0.095	0.066	0.045	0.054	0.023	0.076	0.085	0.070	0.060
CV (%)	25.0	22.2	23.0	15.5	43.7	57.7	34.9	28.4	9.3	11.0	8.6	7.8
C_S	−0.033	−0.651	−0.113	−0.852	0.491	0.666	0.535	1.166	−0.287	0.635	0.100	0.649
C_K	−1.386	−1.501	−1.108	−1.714	−0.297	0.693	−0.104	2.177	−1.154	−0.949	−1.663	−1.836

6 Conclusions

The paper described the procedures involved in the prediction of the variables, viz., K_L, K_r, and K_t adopting MLP and RBF networks. The performance of these networks was evaluated by GoF test using KS test statistic and model performance analysis using MPIs. From the results of data analysis, the following conclusions were drawn from the study:

(i) Optimum MLP network architecture, viz., 12-15-1 was used for training the network.
(ii) KS test results supported the use of both MLP and RBF networks in evaluating the hydrodynamic characteristics parameters.
(iii) Qualitative assessment through time series and scatter plots indicated that the fitted curves using MLP is closer to the fitted curves of the experimental data.
(iv) Model performance analysis indicated the MLP is better suited amongst two networks adopted for prediction of K_L, K_r and K_t.
(v) For K_L, the values of CC, MAE, and MEF given by MLP were found to be 0.994, 1.2% and 98.8% respectively during the testing period. Similarly, the values of CC, MAE, and MEF were computed as 0.968, 0.9%, and 97.7%, respectively, for K_r. For K_t, the values of CC, MAE, and MEF were computed as 0.998, 0.5%, and 99.5%.
(vi) The study suggested that the predicted variable of K_L, K_r and K_t by MLP network could be considered for evaluation of the hydrodynamic performance of QBW.

Acknowledgements The authors are grateful to Dr. (Mrs.) V. V. Bhosekar, Additional Director and Director In-charge, Central Water and Power Research Station, Pune, for providing research facilities to carry out the study. The authors are thankful to National Institute of Technology, Surathkal, for the supply of experimental data used in the study.

References

1. Amr HE, El-Shafie A, Hasan GE, Shehata A, Taha MR (2011) Artificial neural network technique for rainfall forecasting applied to Alexandria. Int J Phys Sci 6(6):1306–1316
2. Balakrishna K, Hegde AV (2015) Reflection and dissipation characteristics of non-overtopping quarter circle breakwater with low-mound rubble base. J Adv Res Ocean Eng 1(1):44–054
3. Binumol S, Rao S, Hegde AV (2015) Runup and rundown characteristics of an emerged seaside perforated quarter circle breakwater. Aquat Procedia 4(1):234–239
4. Chen J, Adams BJ (2006) Integration of artificial neural networks with conceptual models in rainfall-runoff modelling. J Hydrol 318(1–4):232–249
5. D'Agostino BR, Stephens AM (1986) Goodness-of-fit techniques. M/s Marcel Dekkar Inc., New York 10016, USA
6. Deshpandey RR (2012) On the rainfall time series prediction using multilayer perceptron artificial neural network. Int J Emerg Technol Adv Eng 2(1):2250–2459
7. Hafeeda V, Binumol S, Hegde AV, Rao S (2014) Wave reflection by emerged sea side perforated quarter circle breakwater. Int J Earth Sci Eng 7(2):454–460

8. Hegde AV, Ravikiran L (2013) Wave structure interaction for submerged quarter circle breakwaters of different radii-reflection characteristics. World Acad Sci Eng Technol 7(7):1367–1371
9. Jiang XL, Gu HB, Li YB (2008) Numerical simulation on hydraulic performances of quarter circular breakwater. China Ocean Eng 22(4):585–594
10. Kaltech M (2008) Rainfall-runoff modelling using artificial neural networks: modelling and understanding. J Environ Sci 6(1):53–58
11. Karthik S, Rao S (2017) Application of soft computing in breakwater studies—a review. Int J Innov Res Sci Eng Technol 6(5):8355–8359
12. Shao LM (2003) Separation of incident waves and reflected waves and study of reflection coefficient. Dalian University of Technology Press, Dalian (in Chinese)
13. Shi YJ, Wu Mi-Ling, Xue-Lian Jiang, Yan-bao Li (2011) Experimental research on reflection and transmitting performance of quarter circle breakwater under regular and irregular waves. China Ocean Eng 25(3):469–478
14. Tokar S, Markus M (2000) Precipitation runoff modelling using artificial neural network and conceptual models. J Hydrol Eng 5(2):156–161
15. Xie SL, Li YB, Wu YQ, Gu HB (2006) Preliminary research on wave forces on quarter circular breakwater. Ocean Eng 24(1):14–18